Upregulation of osteoprotegerin inhibits *tert*-butyl hydroperoxide-induced apoptosis of human chondrocytes

QIFENG REN[1*], WENFEI ZHANG[2*], PING LI[3], JIANLI ZHOU[4], ZHONGHAO LI[1], YANG ZHOU[5] and MING LI[1]

Departments of [1]Joint Surgery, [2]Clinical Psychology, [3]Hematology and [4]Nuclear Medicine, Dezhou People's Hospital, Dezhou, Shandong 253014; [5]Central Laboratory, Zhongshan Hospital of Xiamen University, School of Medicine, Xiamen University, Xiamen, Fujian 361004, P.R. China

Received September 9, 2021; Accepted March 31, 2022

DOI: 10.3892/etm.2022.11397

Abstract. Necrosis of the femoral head (NFH) is an orthopedic disease characterized by a severe lack of blood supply to the femoral head and a marked increase in intraosseous pressure. NFH is associated with numerous factors, such as alcohol consumption and hormone levels. The present study focused on the expression levels of osteoprotegerin (OPG) in NFH and the effect of *OPG* overexpression on chondrocyte apoptosis. The results demonstrated that *OPG* expression was markedly decreased in the femoral head of patients with NFH compared with normal femoral heads. Lentivirus-mediated overexpression of *OPG* in human chondrocytes reversed the decrease in cell viability and the increase in reactive oxygen species production induced by an oxidative stress-inducing factor, *tert*-butyl hydroperoxide. Flow cytometry and TUNEL assays revealed that *OPG* overexpression inhibited the apoptosis of chondrocytes. In addition, it was revealed that *OPG* exerted its anti-apoptotic effect mainly by promoting Bcl-2 expression and Akt phosphorylation and inhibiting caspase-3 cleavage and Bax expression. The present study revealed that *OPG* may be an important regulator of NFH.

Correspondence to: Dr Yang Zhou, Central Laboratory, Zhongshan Hospital of Xiamen University, School of Medicine, Xiamen University, 201-209 Hubinnan Road, Siming, Xiamen, Fujian 361004, P.R. China
E-mail: zhouyang001001@163.com

Professor Ming Li, Department of Joint Surgery, Dezhou People's Hospital, 1166 Dongfanghong West Road, Decheng, Dezhou, Shandong 253014, P.R. China
E-mail: gklm1628@163.com

[*]Contributed equally

Key words: osteoprotegerin, necrosis of the femoral head, apoptosis, chondrocytes, *tert*-butyl hydroperoxide

Introduction

Necrosis of the femoral head (NFH) is an orthopedic disease that results in a decrease in blood supply to the femoral head under the joint action of numerous factors. This leads to the apoptosis or death of cartilage cells and a decrease in the number of osteocytes, which reduces the mechanical strength of the femoral head (1,2). Finally, the femoral head collapses, resulting in functional disorders of the hip joint (3). Although a number of studies have investigated the etiology, pathology and pathogenesis of NFH, the exact pathogenesis and related risk genes remain unclear (4-7). Therefore, it is important to identify regulatory genes and targets to improve the understanding of the molecular pathological mechanism of this disorder.

Osteoprotegerin (OPG) belongs to the tumor necrosis factor receptor superfamily, members of which are implicated in multiple functions, including blocking osteoclast maturation, controlling vascular calcification, and promoting tumor growth and metastasis (8). A large number of studies have suggested that the competitive binding between OPG and its ligand, OPGL, is the most important regulatory mechanism in the process of osteoclast differentiation, proliferation, apoptosis and physiological function (9-11). There is increasing evidence that OPG not only protects bone but also inhibits apoptotic factors and possibly vasoprotective and cytoprotective factors (4,12-15). The expression of OPG has been detected in xenogeneic antigen-extracted cancellous bone/lentiviral basic fibroblast growth factor/mesenchymal stem cell transplantation for the repair of rabbit femoral head defect necrosis (16). Chondrocytes have been demonstrated to be an ideal material for studying the biological role of OPG in NFH (2). Small molecules can diffuse from the bone marrow through the subchondral bone and deep layers of cartilage to the synovial fluid (17). OPG expressed by chondrocytes is capable of binding to certain receptors to prevent the resorption of subchondral bone and protect cartilage from degradation (2). However, the expression of OPG during NFH and its potential anti-apoptotic effect on human chondrocytes are unclear. The present study explored the expression levels of OPG in a large number of tissue samples from patients with NFH and investigated the potential anti-apoptotic effect of OPG in human chondrocytes.

Materials and methods

Case information. The present study was approved by the Ethics Committee of Dezhou People's Hospital (approval no. EC-20210120-1006; Dezhou, China) and was conducted in compliance with the Declaration of Helsinki for medical research involving human subjects. A total of 50 femoral head tissue samples were collected from hospitalized patients in Dezhou People's Hospital (Dezhou, China) who were admitted between October 2012 and October 2015 and diagnosed with steroid- or alcohol-induced NFH by clinical diagnosis and histopathological examination (Table SI). The inclusion criteria were as follows: i) Volunteered to participate in the study and agreed to take femoral head tissues; ii) met the diagnostic criteria of NFH; iii) aged ≥18 years old; iv) subjects were conscious and could communicate correctly; and v) no tumor or other serious physical diseases. Exclusion criteria: i) Aged <18 years old; and ii) suffering from metabolic disease and neuropsychiatric diseases. The age and sex distribution of patients in each group are presented in Table SI. A total of 30 patients without joint or bone disease who underwent treatment for femoral neck fractures at Dezhou People's Hospital (Dezhou, China) volunteered to donate femoral head tissues for the control group between March 2013 and December 2018. All samples were obtained from a tissue bank at the hospital.

Hematoxylin-eosin staining. Hematoxylin-eosin (HE) staining is a technical method widely used in pathology research. The femoral head tissues obtained during the operation were fixed in 4% formalin for 48 h at room temperature and then embedded in paraffin. The specific steps of HE staining were as follows: i) Dewaxing: Dried 4-μm-thick slices were immediately placed in xylene for dewaxing for 5-10 min at room temperature, then placed into gradient alcohol (100, 90, 80, 70 and 0%) for 2 min for each step, and then moved into water for ~2 min; ii) staining: Slices were successively transferred into hematoxylin for 8-15 min at room temperature, followed by 1-2 min in water at room temperature. They were transferred into differentiation solution (1 ml hydrochloric acid with 99 ml 70% alcohol) and differentiation was allowed to occur for 1-30 sec at room temperature. The slices were moved into water and washed for 30-60 min at room temperature to make the tissues appear dark blue in a light microscope. The slices were transferred into eosin solution and soaked for 2-5 min at room temperature. The eosin floating solution was removed with water and the excess dye on the glass slide was wiped away with gauze; iii) dehydration: Samples were sliced 4-μm thick and placed in 80% alcohol (1-2 min), 90% alcohol (2-4 min) and 100% ethanol (4-8 min); iv) permeabilization: The slices were transferred into xylene for permeabilization for 3-5 min. Then, the xylene was replaced and permeabilized the aforementioned slices again for 5-10 min; and v) Sealing: First, the slices were removed from the xylene, the xylene around the tissue slice was quickly wiped off, and then a drop of neutral gum was dropped on the tissue slice. A clean cover glass was taken, carefully aligned, added to the sealing agent and flattened slowly, and the sample was dried at room temperature.

Cell culture and lentiviral infection of chondrocytes. Small pieces of cartilage tissue were taken from the joint surface during surgery, washed with PBS three times, cut into 1-mm^3 pieces and transferred to a small conical bottle. To digest the tissue samples, these were incubated with 0.5 ml 2% type II collagenase and digested at 37˚C for 45 min. Free chondrocytes in the enzyme solution were filtered through a 120-mesh nylon filter using a pipette (18). The obtained filtrate was transferred to a sterile centrifuge tube and centrifuged at 1,200 x g for 8 min at room temperature. The resulting supernatant was discarded and, to terminate the digestion reaction, 5 ml DMEM (Gibco; Thermo Fisher Scientific, Inc.) containing 10% FBS (Gibco; Thermo Fisher Scientific, Inc.) was added and the samples were mixed. The chondrocyte suspension was then diluted to $3x10^5$ cells/ml and inoculated into a culture dish containing DMEM/F12 (Gibco; Thermo Fisher Scientific, Inc.) with 10% FBS (Gibco; Thermo Fisher Scientific, Inc.) and supplementary antibiotics (50 U/ml penicillin and 50 μg/ml streptomycin) at 37˚C with 5% CO_2 in a humidified atmosphere (18).

Lentiviral transduction was performed in 293T cells (Shanghai Institute of Biochemistry and Cell Biology) by transient co-transfection of a three-plasmid expression system involving an OPG plasmid (pLVX-TRE3G-OPG) or a control plasmid (pLVX-TRE3G) (Shanghai Zeye, Inc.) and the procedure was performed according to the previous reports (19,20). The primary chondrocytes for lentiviral infection were obtained from individuals without joint or bone disease. Primary chondrocytes were cultured in a Petri dish to 80-90% confluence and then trypsinized into a cell suspension (21). The number of cells was adjusted to $1x10^5$ cells per well using culture medium, and the cells were inoculated into 24-well plates and cultured at 37˚C with 5% CO_2 for 24 h. After the cells adhered to the wall of the well, they were ready for transfection. Lentivirus vectors were added to each well at a MOI of 25, 50, 100 or 200. After 72 h of culture, fluorescent protein expression was observed in the cells under an inverted fluorescence microscope, and the virus infection efficiency was calculated. Cells with a transfection efficiency of 80% (MOI=100) were selected for follow-up experiments (data not shown).

RT-qPCR assay. Total RNA was extracted from the primary chondrocytes and cartilage tissues using TRIzol® reagent (Thermo Fisher Scientific, Inc.) and then reverse transcribed into cDNA using a PrimeScript™ RT reagents kit (Takara Bio, Inc.) according to the manufacturer's instructions. qPCR reactions were performed using a KAPA SYBR® FAST qPCR Kit (Kapa Biosystems; Roche Diagnostics) and a CFX96 real-time PCR system (Bio-Rad Laboratories, Inc.). The OPG-specific primers used were: 5'-CATTCTTCAGGTTTGCTGTTCCT-3' (forward) and 5'-TTGCCGTTTTATCCTCTCTACACTC-3' (reverse). GAPDH was used as an internal reference gene for the RT-qPCR experiments, and the primers used were: 5'-CAA TGACCCCTTCATTGACC-3' (forward) and 5'-TTGATTTTG GAGGGATCTCG-3' (reverse). The RT-qPCR conditions were as follows: Pre-denaturation at 95˚C for 10 min, then at 95˚C for 10 sec and at 60˚C for 60 sec, repeating for 40 cycles (22,23). OPG expression was normalized to GAPDH and was presented as a relative expression ratio ($2^{-\Delta\Delta Cq}$; $\Delta Cq=Cq_{OPG}-Cq_{GAPDH}$) (24).

MTT assay of cell viability. After infection with lentivirus for 72 h, 200 μl cell suspension was transferred into 96-well plates

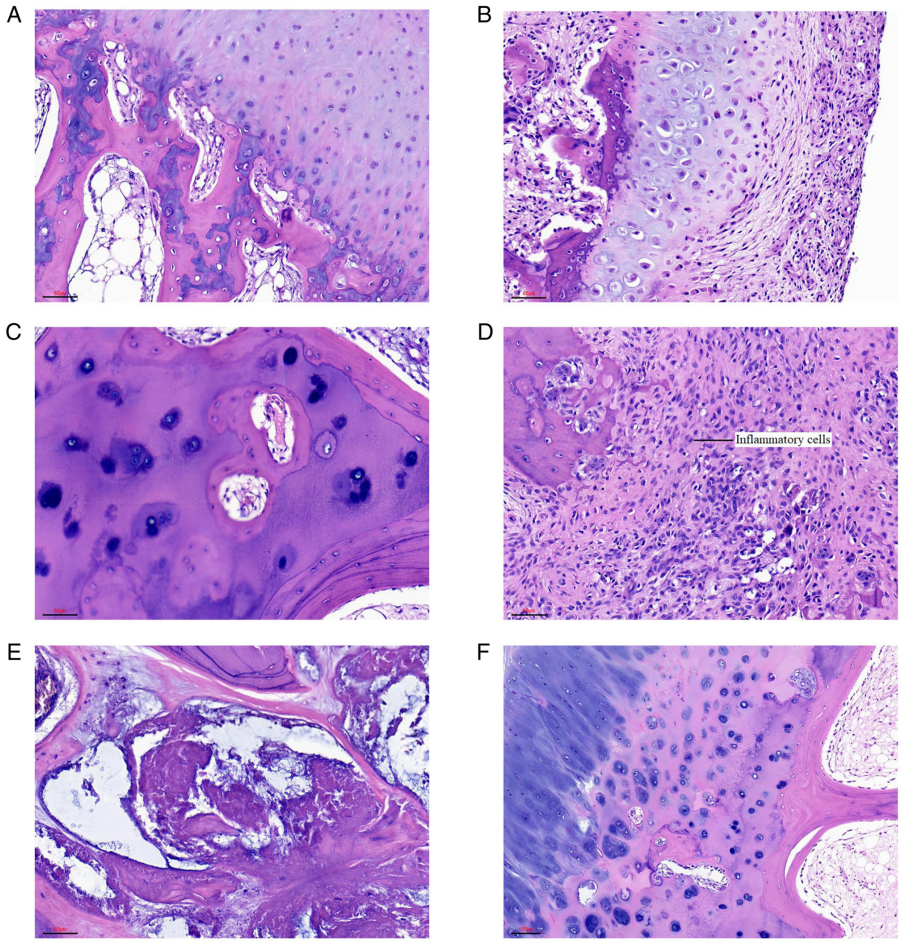

Figure 1. Hematoxylin and eosin staining of femoral head tissue. (A) Normal cartilage. (B) Full anomaly layer. (C) Abnormal metaplasia. (D) Abnormal multinucleated giant cells. (E) Abnormal cystic lesions. (F) Abnormal cartilage hyperplasia. Scale bar, 60 μm.

at a density of 4,000-5,000 cells per well. Preliminary experiments revealed that *tert*-butyl hydroperoxide (tBHP) exerted a significant biological effect on cell viability at a minimum concentration of 100 μM and at a minimum time of 1 day (Figs. S1 and S2). Under these conditions, the interference of other factors on the experimental results can be eliminated to the greatest extent. After 12 h of cell culture, the cells were treated with a final concentration of 100 μM tBHP for 24 h. The cells were then treated with 10 μl 5 mg/ml MTT at 37˚C for an additional 4 h. After removing the culture medium, dimethyl sulfoxide (150 μl) was added to dissolve the formazan crystals. The optical density values of the samples were determined using a microplate spectrophotometer (BioTek Instruments, Inc.) at 490 nm wavelength.

Flow cytometric analysis of apoptosis. Human chondrocytes infected with virus particles containing the OPG plasmid or control plasmid were treated with 100 μM tBHP or vehicle for 24 h at 37˚C. Human chondrocytes were harvested with ethylenediaminetetraacetic acid-free trypsin, washed with PBS and then incubated in 100 μl binding buffer containing 20 μg PI and 5 μl Annexin V-FITC (R&D Systems, Inc.) at 4˚C in the dark for 15 min. Binding buffer (900 μl) was then added and the fluorescence of Annexin V-FITC and PI was detected using a Gallios Flow Cytometer (Beckman Coulter, Inc.). Data were analyzed using FlowJo software v7.6.1 (FlowJo LLC). Cells positive for Annexin V-FITC and negative for PI were considered to be early apoptotic, and cells positive for both Annexin V-FITC and PI were considered to be late apoptotic, whereas those positive for PI and negative for Annexin V-FITC were considered to be necrotic.

TUNEL assay. A terminal deoxynucleotidyl transferase (TdT) -mediated dUTP nick-end labeling (TUNEL) kit (Beyotime Institute of Biotechnology) was used to detect DNA fragmentation resulting from apoptosis according to the manufacturer's instructions. Briefly, terminal deoxynucleotidyl transferase was used to incorporate residues of digoxigenin nucleotide into the 3' OH ends of DNA fragments. The DNA breaking points (nicks) expose the 3' OH-end of DNA, which were labelled, thus allowing the identification of apoptotic cells. Human chondrocytes infected with virus particles were seeded on coverslips and incubated in culture medium containing tBHP (100 μM) for 24 h. After incubation in PBS with 0.2% Triton X-100 for 5 min, the cells were fixed with 4% paraformaldehyde at room temperature for 20 min. The cells were then treated with a mixture of terminal deoxynucleotidyl transferase enzyme, terminal deoxynucleotidyl transferase reaction buffer and fluorescent labeling buffer (1:24:25) for 60 min at 37˚C. DAPI staining (100 ng/ml, 25˚C, 20 min) was used to count the total number of cells, and apoptotic cells were identified as those with green nuclei. Apoptotic cells were

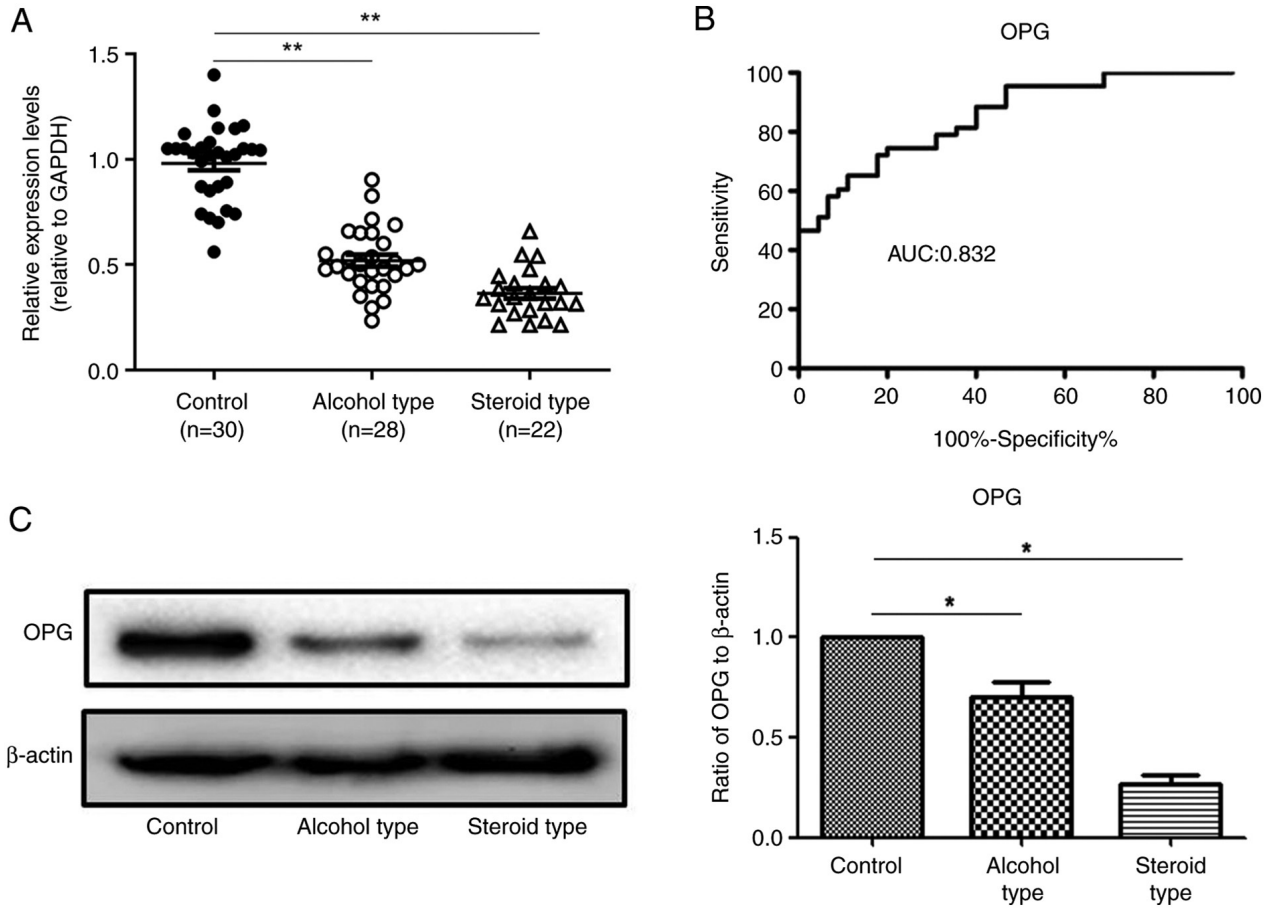

Figure 2. Expression levels of OPG in patients with NFH. (A) Reverse transcription-quantitative PCR detection of OPG in femoral head tissues of normal subjects and patients with NFH (control vs. patients with NFH). (B) Receiver operating characteristic analysis of OPG expression in patients with NFH. (C) Representative western blots of OPG in tissues from controls and patients with NFH, and semi-quantitative analysis of OPG expression (n=30 for control; n=28 for alcohol type; n=22 for steroid type). *P<0.05, **P<0.01. AUC, area under the curve; NFH, necrosis of the femoral head; OPG, osteoprotegerin.

quantitated by counting the number of TUNEL-positive cells in four random microscopic fields of a DM2500 fluorescence microscope (Leica Microsystems GmbH).

Flow cytometric detection of intracellular reactive oxygen species (ROS). To measure ROS production, human chondrocytes infected with virus particles containing the OPG plasmid or control virus particles were cultured in the presence or absence of 100 μM tBHP. After treatment, the cells were incubated with 10 μM 2'-7'-dichlorofluorescin diacetate for 30 min at 37˚C and intracellular ROS levels were determined using a Gallios Flow Cytometer with Kaluza analysis software v2.1.1 (Beckman Coulter, Inc.).

Western blotting. Membrane protein levels were determined by western blotting as described previously (15). Briefly, cells or tissue fragments were lysed with modified RIPA buffer (Beyotime Institute of Biotechnology) for 30 min at 4˚C, and the lysates were then centrifuged at 12,000 x g for 30 min at 4˚C. After transferring the supernatant to a fresh ice-cold tube, the protein concentration was determined using a bicinchoninic acid protein assay kit (Beyotime Institute of Biotechnology). Equal concentrations of proteins were mixed with SDS sample buffer, denatured at 95˚C for 5 min and a total of 40 μg protein was loaded per lane and resolved on 8% SDS-polyacrylamide gel. The separated proteins were then transferred onto nitrocellulose membranes, which were blocked with 5% non-fat dried milk in TBS with 0.1% Tween-20 (TBST) at room temperature for 1 h. After blocking, the blots were incubated overnight at 4˚C with the primary antibodies (dilution, 1:1,000). The membranes were then washed with TBST and incubated with horseradish peroxidase-conjugated secondary antibodies (1:5,000; ProteinTech Group, Inc.) for 1 h at room temperature. The membranes were washed again with TBST and then processed using an enhanced chemiluminescence detection system (Beyotime Institute of Biotechnology). Relative band intensities were measured using Gel-Pro Analyzer image analysis software v4.5 (Media Cybernetics, Inc.). The antibody details are presented in Table SII.

Statistical analysis. Preliminary experiments revealed no significant difference in results between a blank control and the negative control (pLVX-TRE3G) (Figs. S3 and S4). All experiments were performed in triplicate. Data are presented as the mean ± standard error of the mean, and statistical differences among groups were further evaluated by one-way ANOVA followed by Bonferroni's post hoc test for multiple groups. An unpaired Student's t-test was used to compare two groups. The categorical data were analyzed using chi-squared test (χ^2 test). A receiver operating characteristic (ROC) curve was constructed by calculating the sensitivity

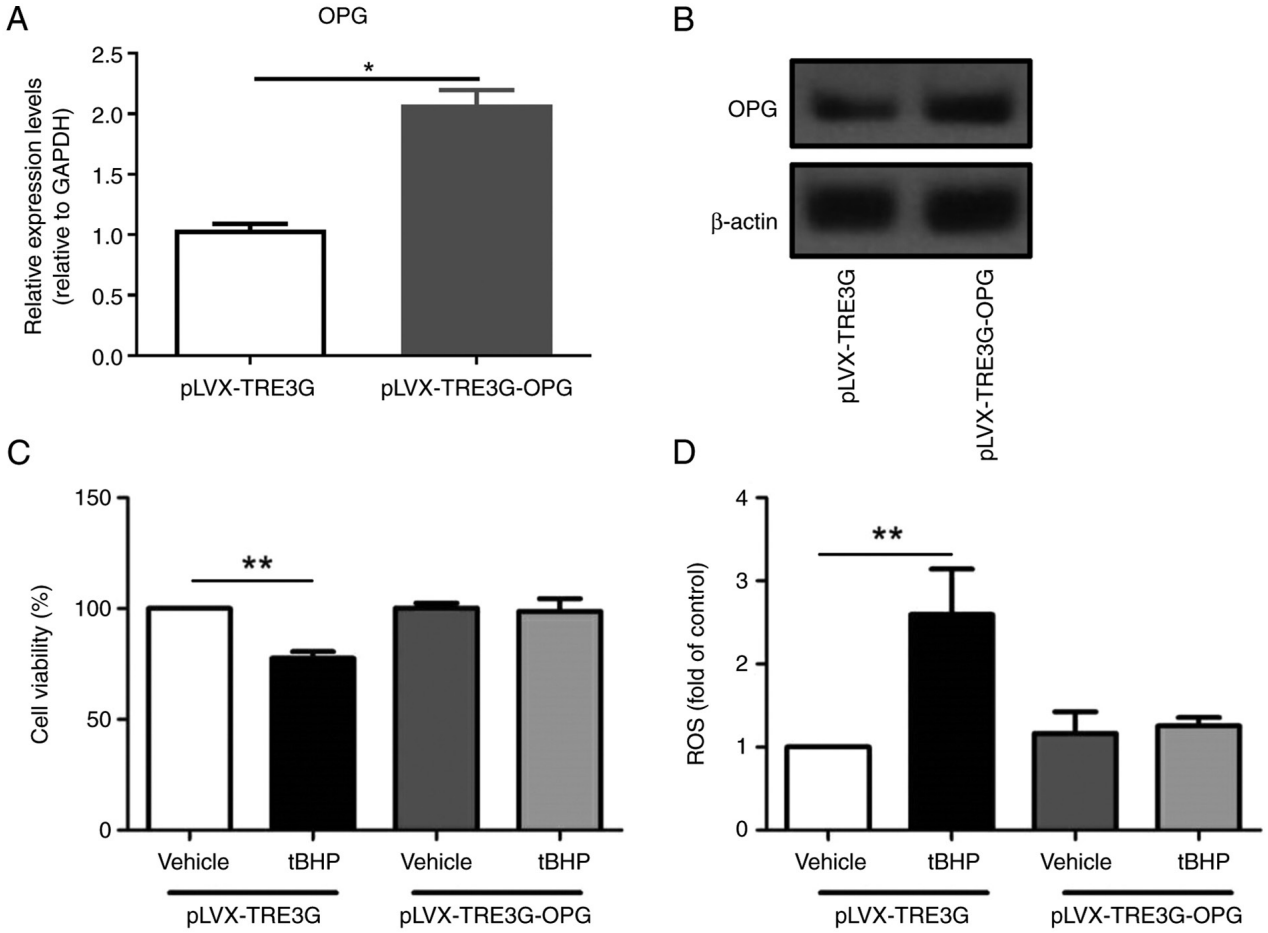

Figure 3. Effects of OPG on chondrocyte viability and ROS production. (A) Increased mRNA level of OPG in the cells transfected with the OPG plasmid compared with cells transfected with the control plasmid (pLVX-TRE3G). (B) The cells transfected with the OPG plasmid showed higher OPG protein level compared with that in cells transfected with the pLVX-TRE3G. (C) Cell viability was determined using an MTT assay in human chondrocytes transfected with OPG or the pLVX-TRE3G only. (D) ROS levels were determined via flow cytometry in human chondrocytes transfected with OPG or pLVX-TRE3G only. *P<0.05, **P<0.01. OPG, osteoprotegerin; ROS, reactive oxygen species; tBHP, *tert*-butyl hydroperoxide.

and specificity of OPG expression in a logistic regression model at different cut-off points to differentiate patients with NFH from controls (25-27). The area under the curve (AUC) can be statistically interpreted as the probability of correctly distinguishing patients with NFH from controls (25-27). All statistical analyses were calculated using SPSS software 17.0 (SPSS Inc.). P<0.05 was considered to indicate a statistically significant difference.

Results

Expression levels of OPG in patients with NFH and their association with NFH. Fig. 1 shows the results of hematoxylin and eosin staining of normal bone, dead bone, infiltrating inflammatory cells and femoral head tissues in patients with steroid-induced NFH and alcoholic NFH. The normal bone color was uniform and smooth (Fig. 1A), whereas the dead bone and steroid-induced femoral head necrotic lesions had blood cells with inflammatory cell infiltration.

RT-qPCR was used to examine *OPG* gene expression in specimens from patients with NFH and those with a normal femoral head. The OPG levels were lower in patients with steroid-(0.31±0.02) or alcohol-induced (0.49±0.06) NFH than in patients with normal femoral heads (1.01±0.12; P<0.05; Fig. 2A). A sensitivity correlation analysis of the ROC curve was performed on *OPG* mRNA expression levels in 50 femoral head samples with necrosis and 30 normal femoral head samples. The AUC for *OPG* expression was 0.832 (95% confidence interval, 0.723-0.881). The cut-off value was 0.452 with sensitivity and specificity values of 85 and 72%, respectively (Fig. 2B). OPG protein expression was also significantly decreased in both alcoholic NFH specimens and steroid-induced NFH specimens compared with normal femoral head specimens (Fig. 2C).

Effect of OPG overexpression on tBHP-induced apoptosis of human chondrocytes. To determine whether OPG has a protective effect on chondrocytes, an MTT assay was performed to examine the viability of tBHP-treated human chondrocytes transfected with OPG or control plasmids. There was a significantly increased mRNA level of OPG in the cells transfected with the OPG plasmid compared with cells transfected with the control plasmid (Fig. 3A). The cells transfected with the OPG plasmid showed higher OPG protein level compared with that in cells transfected with the control plasmid (Fig. 3B). As shown in Fig. 3C, the viability of human chondrocytes transfected with the control plasmid (pLVX-TRE3G) was significantly reduced by ~20% after treatment with 100 μM

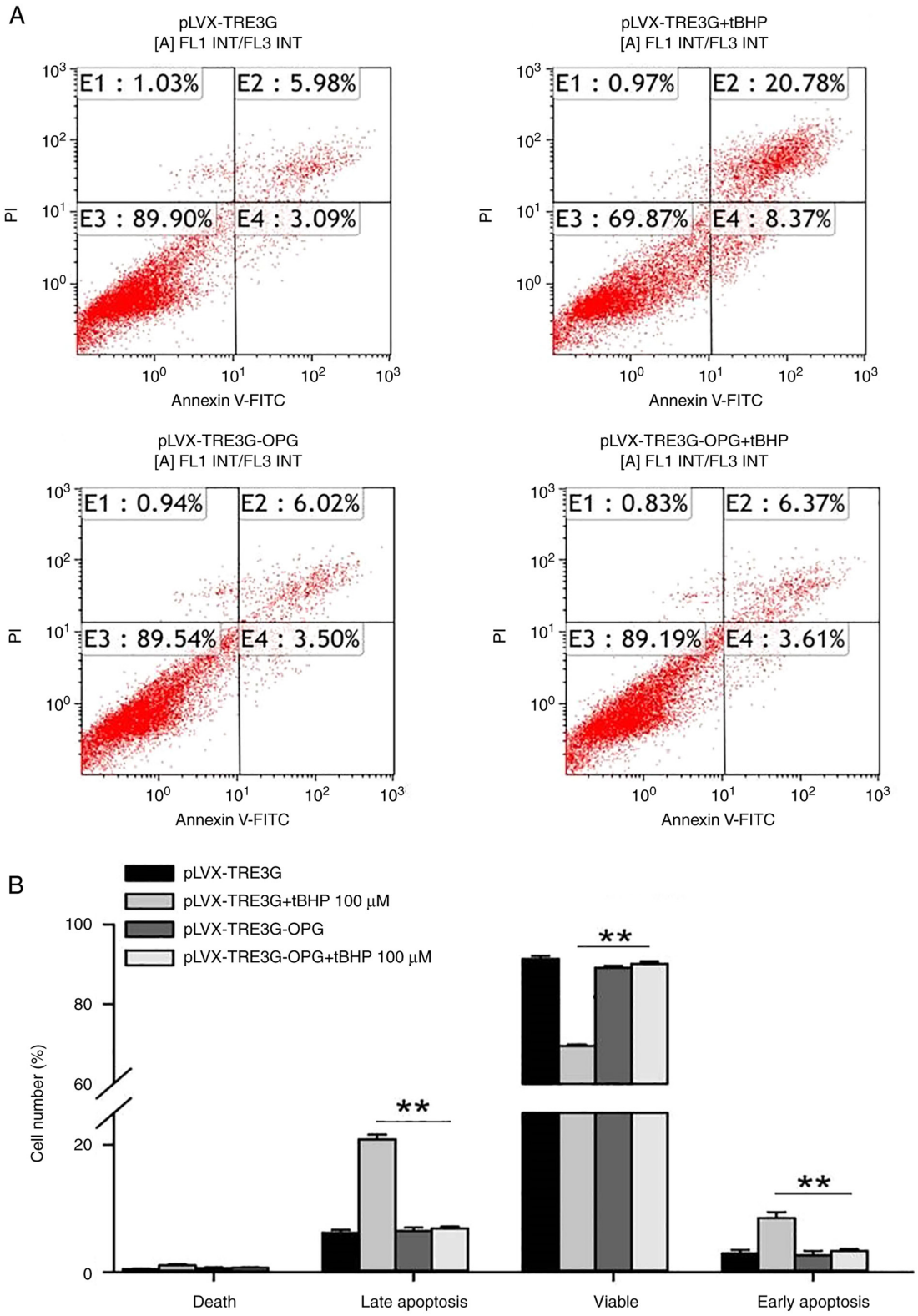

Figure 4. Effects of OPG on tBHP-induced apoptosis of chondrocytes transfected with the OPG plasmid or pLVX-TRE3G. (A) Flow cytometric analysis of cells transfected with OPG plasmid or pLVX-TRE3G only and stained with PI and Annexin V-FITC after incubation with tBHP for 24 h. (B) Percentage of dead cells (E1), those in late apoptosis (E2) and viable cells (E3), and early apoptosis (E4), as analyzed by flow cytometry. **P<0.01. OPG, osteoprotegerin; tBHP, *tert*-butyl hydroperoxide.

tBHP, whereas there was little change in the viability of OPG-transfected chondrocytes (pLVX-TRE3G-OPG). This result indicated that overexpression of OPG in human chondrocytes protects them from tBHP-induced cell death.

Overexpression of OPG suppresses tBHP-induced ROS production in human chondrocytes. ROS are important regulators of cell death and mitochondrial-related apoptosis (28). ROS production in human chondrocytes was detected using

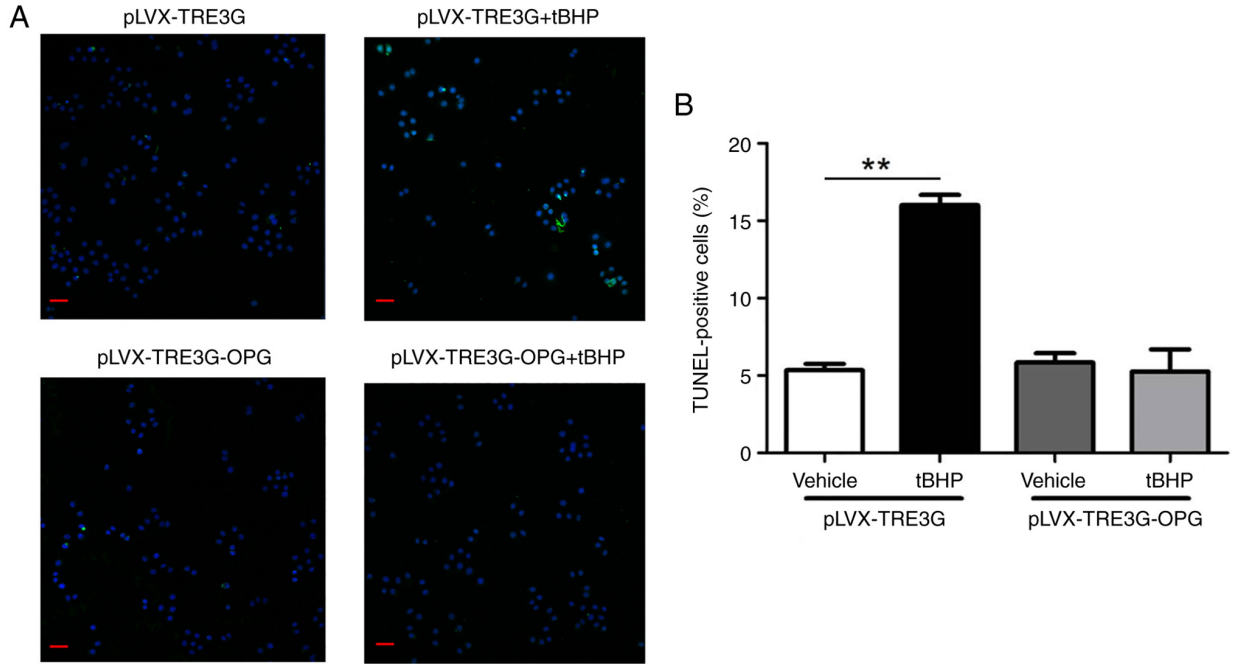

Figure 5. TUNEL assay showing the effects of tBHP on chondrocytes transfected with the OPG plasmid or vector only. (A) Representative microphotographs of TUNEL staining in human chondrocytes transfected with the OPG plasmid or pLVX-TRE3G only. TUNEL-positive cells are green and nuclei labeled with DAPI are blue. (B) Percentage of TUNEL-positive cells. DAPI-stained cells were counted in four random regions. Scale bar, 50 μm. **P<0.01. OPG, osteoprotegerin; tBHP, *tert*-butyl hydroperoxide.

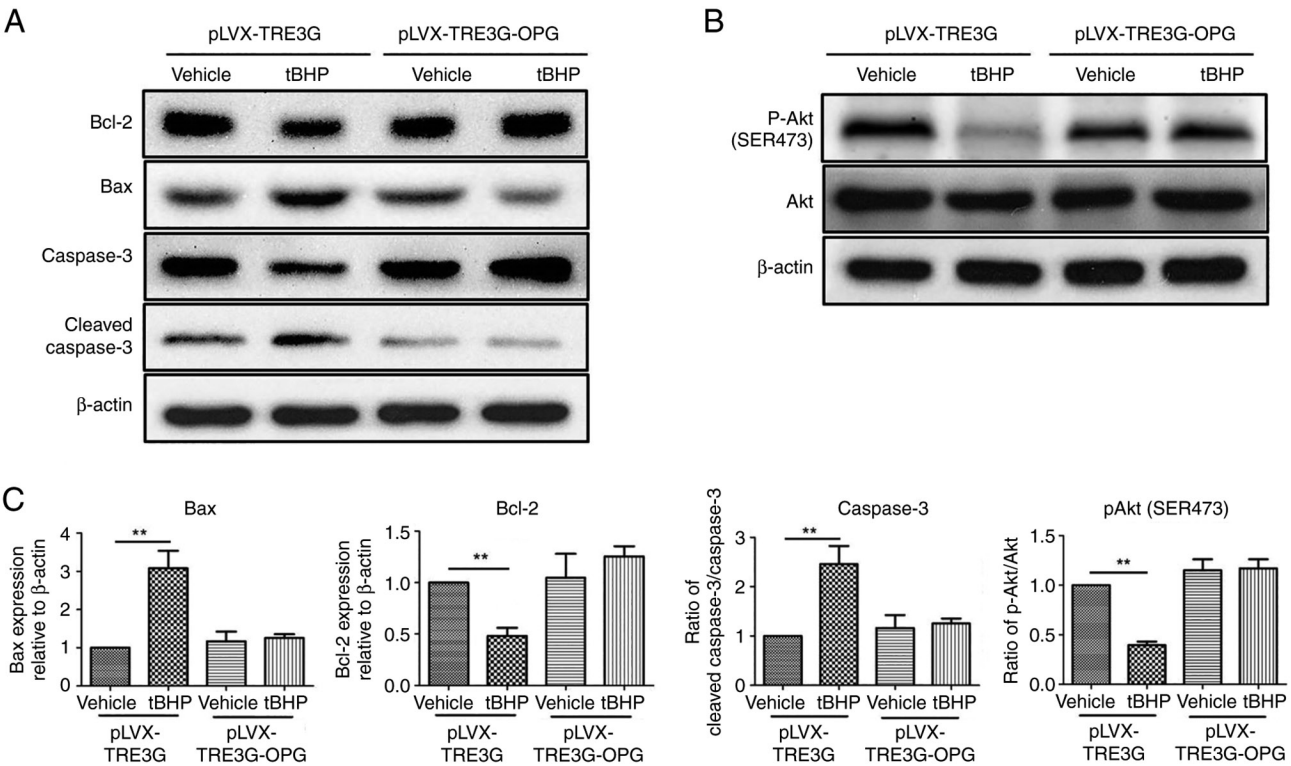

Figure 6. Western blot analysis of apoptosis-related proteins in OPG plasmid-transfected chondrocytes. (A) Western blots of Bax, Bcl-2, caspase-3 and β-actin in human chondrocytes transfected with the OPG plasmid or pLVX-TRE3G only and treated with tBHP or vehicle. (B) Relative levels of p-Akt, Akt and β-actin in human chondrocytes transfected with OPG or vector only, and then treated with vehicle or tBHP for 24 h. (C) Relative levels of Bax, Bcl-2, caspase-3 and p-Akt in human chondrocytes. **P<0.01. OPG, osteoprotegerin; tBHP, *tert*-butyl hydroperoxide; p-, phosphorylated.

flow cytometry. As shown in Fig. 3D, the ROS levels significantly increased after tBHP treatment of human chondrocytes transfected with the pLVX-TRE3G (P<0.01). The representative flow cytometry plots of ROS are shown in Figs. S4 (blank control and negative control: pLVX-TRE3G) and S5 (pLVX-TRE3G, pLVX-TRE3G + tBHP, pLVX-TRE3G-OPG

and pLVX-TRE3G-OPG + tBHP). However, no difference in ROS production was observed between cells overexpressing OPG and tBHP-treated OPG overexpression cells (Fig. 3D).

Overexpression of OPG reduces tBHP-induced human chondrocyte apoptosis. OPG has been demonstrated to have a protective effect against apoptosis (28); however, to the best of our knowledge, there are no reports on the anti-apoptotic effect of OPG in human chondrocytes. In the human chondrocytes with pLVX-TRE3G transfection, tBHP treatment increased the percentage of late apoptotic cells from 5.98±0.36 to 20.78±0.72% and the percentage of early apoptotic cells from 3.09±0.42 to 8.37±0.74% compared with that of the negative control group (pLVX-TRE3G) (Fig. 4A). However, in human chondrocytes transfected with OPG, no significant increase in the number of apoptotic cells was observed after treatment with 100 μM tBHP. Thus, overexpression of OPG significantly inhibited the tBHP-induced apoptosis of human chondrocytes (Fig. 4B, $P<0.01$).

A TUNEL assay was also employed to confirm the tBHP-induced apoptosis of human chondrocytes. As shown in Fig. 5, only ~5% of vehicle-treated human chondrocytes transfected with the pLVX-TRE3G control plasmid were TUNEL-positive, whereas 16% were TUNEL-positive after tBHP treatment. However, only 6% of chondrocytes transfected with *OPG* were TUNEL-positive after tBHP treatment (Fig. 5A and B).

Molecular mechanism of tBHP-induced apoptosis in OPG-overexpressing human chondrocytes. Western blotting was used to explore the expression levels of tBHP-induced apoptosis-related proteins in human chondrocytes overexpressing OPG. As shown in Fig. 6, tBHP increased the levels of the pro-apoptotic proteins Bax (310%) and cleaved caspase-3 (250%), and decreased the levels of the anti-apoptotic proteins Bcl-2 (0.45) and phosphorylated (p-) Akt (0.41), in the vector control group. In human chondrocytes overexpressing OPG, tBHP treatment had no effect on the levels of Bax, cleaved caspase-3, Bcl-2 and p-Akt. This result indicated that overexpression of *OPG* in human chondrocytes inhibited Bax expression and caspase-3 cleavage and promoted Bcl-2 expression and Akt phosphorylation.

Discussion

OPG, also known as osteoclastogenesis inhibitory factor, is a cytokine receptor of the TNF receptor superfamily encoded by the TNF receptor superfamily member 11B gene (2). In the present study, OPG gene expression in the femoral head tissue of patients with steroid-induced NFH and alcoholic NFH was determined by RT-qPCR. The results demonstrated that OPG expression was markedly decreased in patients with steroid-induced and alcoholic NFH compared with normal controls without NFH. Apoptosis can be divided into early apoptosis, characterized by changes in cell membrane structure and phosphatidylserine eversion, early-to-middle apoptosis, characterized by an increase in cytoplasmic density, disappearance of mitochondrial membrane potential, changes in permeability and a release of cytochrome C into the cytoplasm, middle-to-late apoptosis, characterized by apoptosis-related signal transduction, and late apoptosis, characterized by DNA degradation into 180-200 bp fragments (29,30). Recent studies have suggested that the downregulation of OPG expression in patients with NFH may interfere with the differentiation of osteoclasts and their secretory function in the transversing axis of bone remodeling and the inhibition of bone resorption, thus weakening their protective effect on cartilage and causing osteosclerosis and orthopedic diseases, such as osteoporosis (31-36).

OPG is synthesized by osteoblasts and stromal cells and it regulates osteoclast differentiation and activity (37). It can directly affect the differentiation and efficacy of osteoclasts and regulate bone remodeling (35,36,38). The secretory system adjacent to the horizontal axis is involved in bone resorption (39). OPG has a regulatory effect on bone and it protects cartilage (40). It can also participate in the development of a series of orthopedic diseases, such as osteoporosis, osteosclerosis and bone tumors, in combination with receptor activator of NF-κB ligand (RANKL), and it has been demonstrated to serve an important role in bone diseases (41). OPG was first discovered as a novel secreted tumor necrosis factor receptor-related protein that served a role in the regulation of bone density, and it was later found to be a decoy receptor for RANKL (28,42). OPG also binds to TNF-related apoptosis-inducing ligand (TRAIL) and inhibits the TRAIL-induced apoptosis of specific cells, including tumor cells (43). Other OPG ligands include syndecan-1, glycosaminoglycans, von Willebrand factor and the factor VIII-von Willebrand factor complex (44). OPG-knockout (OPG-KO) mice show decreased chondrocyte proliferation and increased chondrocyte apoptosis (1,40). The isolated chondrocytes from OPG-KO mice also show impaired survival and increased chondrogenic differentiation (1,40). Numerous studies have reported that OPG has anti-apoptotic effects (3,45). In addition to severe osteoporosis and multiple fractures, OPG-KO mice also have calcification in the middle layers of the aorta and renal arteries (8). In the bone marrow mesenchymal stem cells, OPG has been found to inhibit TRAIL-induced apoptosis (46). OPGα or β3 can prevent the apoptosis of rat aortic endothelial cells and human capillary endothelial cells, and the anti-apoptotic effect of OPG is further achieved by activating NF-κB to increase OPG expression (42). In the osteoclasts, OPG regulates apoptosis via Bcl-2/Bax and caspase-3 in the classic Fas/Fas ligand apoptosis pathway (47). A previous study has demonstrated that OPG inhibits the apoptosis of human mammary epithelial cells, in part because it blocks the binding of TRAIL to death receptors, and the apoptosis of endothelial cells, in which high expression levels of OPG and vascular endothelial growth factor are more viable (48).

In the absence of OPG, mice show thinned articular cartilage and extensive remodeling of the subchondral bone in the femoral head (2). The articular cartilage also shows decreased levels of aggrecan, collagen (Col)-II and Col-X, but increased levels of Col-I and matrix metalloproteinase-13 in the femoral head of OPG-KO mice compared with wild-type mice (2). Furthermore, OPG-KO mice have increased chondrocyte apoptosis and decreased chondrocyte proliferation in the femoral head compared with wild-type mice (2). Additionally, the present study demonstrated that overexpression of OPG in human chondrocytes by lentivirus-mediated transfection inhibited the decrease in cell viability induced by tBHP. The present study revealed that increasing OPG expression could inhibit the production of ROS caused by tBHP. Since ROS is a

key stimulator related to apoptosis (28), this strongly suggested that OPG might be involved in the process of apoptosis. Further investigation revealed that this effect of OPG occurred by inhibiting late and early apoptosis. Furthermore, the present study investigated apoptosis-related signaling pathways and revealed that overexpression of OPG increased Bcl-2 expression and Akt phosphorylation levels and decreased the levels of Bax and cleaved caspase-3. The present results are also consistent with those reported by other groups (8,17,49,50). Cheng *et al* (51) found that graphene oxide nanoparticles may be used to protect cartilage by modifying the RANKL/OPG axis. This line of evidence suggests that OPG is essential for maintaining the physiological function of chondrocytes in the femoral head.

In summary, the present study revealed that the expression levels of OPG were lower in femoral heads from patients with NFH than those from control patients. Overexpression of OPG decreased tBHP-induced cell death, cellular ROS production and late and early apoptosis by inhibiting Bax and cleaved caspase-3 and promoting Bcl2 expression and Akt phosphorylation in human chondrocytes. The present study provides novel strategies for the clinical treatment and basic research of NFH.

Acknowledgements

Not applicable.

Funding

This work was supported by the Medical and Health Science and Technology Development Program of Shandong Province (grant no. 2019ws015).

Availability of data and materials

The datasets used and/or analyzed during the current study are available from the corresponding author on reasonable request.

Authors' contributions

YZ and ML conceived and designed the study. QR, WZ, PL, JZ and ZL performed the study experiments. YZ and ML wrote the paper. All authors have read and approved the final manuscript. QR, YZ and ML confirm the authenticity of all the raw data.

Ethics approval and consent to participate

All procedures in the present study were approved by the Medical Ethics Committee of Dezhou People's Hospital (Dezhou, China) and written informed consent was obtained from all subjects.

Patient consent for publication

Not applicable.

Competing interests

The authors declare that they have no competing interests.

References

1. Chen D, Liu Y, Liu Z and Wang P: OPG is required for the postnatal maintenance of condylar cartilage. Calcif Tissue Int 104: 461-474, 2019.
2. Liu Y, Ge J, Chen D, Weng Y, Du H, Sun Y and Zhang Q: Osteoprotegerin deficiency leads to deformation of the articular cartilage in femoral head. J Mol Histol 47: 475-483, 2016.
3. Bouredji Z, Hamoudi D, Marcadet L, Argaw A and Frenette J: Testing the efficacy of a human full-length OPG-Fc analog in a severe model of cardiotoxin-induced skeletal muscle injury and repair. Mol Ther Methods Clin Dev 21: 559-573, 2021.
4. Manolagas SC, O'Brien CA and Almeida M: The role of estrogen and androgen receptors in bone health and disease. Nat Rev Endocrinol 9: 699-712, 2013.
5. Al-Omari AA, Aleshawi AJ, Marei OA, Younes HMB, Alawneh KZ, ALQuran E and Mohaidat ZM: Avascular necrosis of the femoral head after single steroid intra-articular injection. Eur J Orthop Surg Traumatol 30: 193-197, 2020.
6. Wang T, Azeddine B, Mah W, Harvey EJ, Rosenblatt D and Séguin C: Osteonecrosis of the femoral head: Genetic basis. Int Orthop 43: 519-530, 2019.
7. Lee SW, Lim KH, Lee KJ, Heo YR and Lee JH: No association between telomere length and osteonecrosis of the femoral head. BMC Musculoskelet Disord 22: 176, 2021.
8. Li Y, Guo Y, Wang Q, Ouyang Y, Cao Y, Jin T and Wang J: Osteoprotegerin polymorphisms are associated with alcohol-induced osteonecrosis of femoral head in Chinese Han population from Henan province. J Genet 95: 983-989, 2016.
9. Hardy R, Juarez M, Naylor A, Tu J, Rabbitt EH, Filer A, Stewart PM, Buckley CD, Raza K and Cooper MS: Synovial DKK1 expression is regulated by local glucocorticoid metabolism in inflammatory arthritis. Arthritis Res Ther 14: R226, 2012.
10. Holt V, Caplan AI and Haynesworth SE: Identification of a subpopulation of marrow MSC-derived medullary adipocytes that express osteoclast-regulating molecules: Marrow adipocytes express osteoclast mediators. PLoS One 9: e108920, 2014.
11. Walsh MC and Choi Y: Biology of the RANKL-RANK-OPG system in immunity, bone, and beyond. Front Immunol 5: 511, 2014.
12. Kuhn MC, Willenberg HS, Schott M, Papewalis C, Stumpf U, Flohé S, Scherbaum WA and Schinner S: Adipocyte-secreted factors increase osteoblast proliferation and the OPG/RANKL ratio to influence osteoclast formation. Mol Cell Endocrinol 349: 180-188, 2012.
13. Liu Y, Berendsen AD, Jia S, Lotinun S, Baron R, Ferrara N and Olsen B: Intracellular VEGF regulates the balance between osteoblast and adipocyte differentiation. J Clin Invest 122: 3101-3113, 2012.
14. Milanova V, Ivanovska N and Dimitrova P: TLR2 elicits IL-17-mediated RANKL expression, IL-17, and OPG production in neutrophils from arthritic mice. Mediators Inflamm 2014: 643406, 2014.
15. Cheng J, Zhuo H, Wang L, Zheng W, Chen X, Hou J, Zhao J and Cai J: Identification of the combinatorial effect of miRNA family regulatory network in different growth patterns of GC. Mol Ther Oncolytics 17: 531-546, 2020.
16. Peng W, Zhang J, Zhang F, Zhao Y and Dong W: Expression of osteoprotegerin and receptor activator for the nuclear factor-κB ligand in XACB/LV-bFGF/MSCs transplantation for repair of rabbit femoral head defect necrosis. J Cell Biochem: Oct 18, 2018 (Epub ahead of print).
17. Kovács B, Vajda E and Nagy EE: Regulatory effects and interactions of the Wnt and OPG-RANKL-RANK signaling at the bone-cartilage interface in osteoarthritis. Int J Mol Sci 20: 4653, 2019.
18. Zhou Y, Chen X, Qu N, Zhang B and Xia C: Chondroprotection of PPARα activation by WY14643 via autophagy involving Akt and ERK in LPS-treated mouse chondrocytes and osteoarthritis model. J Cell Mol Med 23: 2782-2793, 2019.
19. Huang M, Thomas D, Li MX, Feng W, Chan SM, Majeti R and Mitchell BS: Role of cysteine 288 in nucleophosmin cytoplasmic mutations: Sensitization to toxicity induced by arsenic trioxide and bortezomib. Leukemia 27: 1970-1980, 2013.
20. Yenerall P, Kollipara RK, Avila K, Peyton M, Eide CA, Bottomly D, McWeeney SK, Liu Y, Westover KD, Druker BJ, *et al*: Lentiviral-driven discovery of cancer drug resistance mutations. Cancer Res 81: 4685-4695, 2021.

21. Cheng L, Zeng G, Liu Z, Zhang B, Cui X, Zhao H, Zheng X, Song G, Kang J and Xia C: Protein kinase B and extracellular signal-regulated kinase contribute to the chondroprotective effect of morroniside on osteoarthritis chondrocytes. J Cell Mol Med 19: 1877-1886, 2015.
22. Yang P, Qiu Z, Jiang Y, Dong L, Yang W, Gu C, Li G and Zhu Y: Silencing of cZNF292 circular RNA suppresses human glioma tube formation via the Wnt/β-catenin signaling pathway. Oncotarget 7: 63449, 2016.
23. Zhong Z, Lv M and Chen J: Screening differential circular RNA expression profiles reveals the regulatory role of circTCF25-miR-103a-3p/miR-107-CDK6 pathway in bladder carcinoma. Sci Rep 6: 30919, 2016.
24. Livak KJ and Schmittgen TD: Analysis of relative gene expression data using real-time quantitative PCR and the 2(-Delta Delta C(T)) method. Methods 25: 402-408, 2001.
25. Gao S, Cheng J, Li G, Sun T, Xu Y, Wang Y, Du X, Xu G and Duan S: Catechol-O-methyltransferase gene promoter methylation as a peripheral biomarker in male schizophrenia. Eur Psychiatry 44: 39-46, 2017.
26. Tian H, Li G, Xu G, Liu J, Wan X, Zhang J, Xie S, Cheng J and Gao S: Inflammatory cytokines derived from peripheral blood contribute to the modified electroconvulsive therapy-induced cognitive deficits in major depressive disorder. Eur Arch Psychiatry Clin Neurosci 271: 475-485, 2021.
27. Cheng J, Zhuo H, Xu M, Wang L, Xu H, Peng J, Hou J, Lin L and Cai J: Regulatory network of circRNA-miRNA-mRNA contributes to the histological classification and disease progression in gastric cancer. J Transl Med 16: 1-14, 2018.
28. Shafiey SI, Mohamed WR and Abo-Saif AA: Paroxetine and rivastigmine mitigates adjuvant-induced rheumatoid arthritis in rats: Impact on oxidative stress, apoptosis and RANKL/OPG signals. Life Sci 212: 109-118, 2018.
29. Carneiro BA and El-Deiry WS: Targeting apoptosis in cancer therapy. Nat Rev Clin Oncol 17: 395-417, 2020.
30. Voss AK and Strasser A: The essentials of developmental apoptosis. F1000Res 9: F1000 Faculty Rev-148, 2020.
31. Tanaka H, Mine T, Ogasa H, Taguchi T and Liang CT: Expression of RANKL/OPG during bone remodeling in vivo. Biochem Biophys Res Commun 411: 690-694, 2011.
32. Upton AR, Holding CA, Dharmapatni AA and Haynes DR: The expression of RANKL and OPG in the various grades of osteoarthritic cartilage. Rheumatol Int 32: 535-540, 2012.
33. Nishida D, Arai A, Zhao L, Yang M, Nakamichi Y, Horibe K, Hosoya A, Kobayashi Y, Udagawa N and Mizoguchi T: RANKL/OPG ratio regulates odontoclastogenesis in damaged dental pulp. Sci Rep 11: 4575, 2021.
34. Guo Y, Xu C, Wu X, Zhang W, Sun Y and Shrestha A: Leptin regulates OPG and RANKL expression in gingival fibroblasts and tissues of chronic periodontitis patients. Int J Med Sci 18: 2431-2437, 2021.
35. Song HM, Wei YC, Li N, Wu B, Xie N, Zhang KM, Wang SZ and Wang HM: Effects of Wenyangbushen formula on the expression of VEGF, OPG, RANK and RANKL in rabbits with steroid-induced femoral head avascular necrosis. Mol Med Rep 12: 8155-8161, 2015.
36. Chen K, Liu Y, He J, Pavlos N, Wang C, Kenny J, Yuan J, Zhang Q, Xu J and He W: Steroid-induced osteonecrosis of the femoral head reveals enhanced reactive oxygen species and hyperactive osteoclasts. Int J Biol Sci 16: 1888-1900, 2020.
37. Hardaway AL, Herroon MK, Rajagurubandara E and Podgorski I: Bone marrow fat: Linking adipocyte-induced inflammation with skeletal metastases. Cancer Metastasis Rev 33: 527-543, 2014.
38. Boyce BF and Xing L: Functions of RANKL/RANK/OPG in bone modeling and remodeling. Arch Biochem Biophys 473: 139-146, 2008.
39. Sakamoto K, Osaki M, Hozumi A, Goto H, Fukushima T, Baba H and Shindo H: Simvastatin suppresses dexamethasone-induced secretion of plasminogen activator inhibitor-1 in human bone marrow adipocytes. BMC Musculoskelet Disord 12: 82, 2011.
40. Shimizu S, Asou Y, Itoh S, Chung UI, Kawaguchi H, Shinomiya K and Muneta T: Prevention of cartilage destruction with intraarticular osteoclastogenesis inhibitory factor/osteoprotegerin in a murine model of osteoarthritis. Arthritis Rheum 56: 3358-3365, 2007.
41. Busillo JM and Cidlowski JA: The five Rs of glucocorticoid action during inflammation: Ready, reinforce, repress, resolve, and restore. Trends Endocrinol Metab 24: 109-119, 2013.
42. Soliman S and Ahmed M: The effect of orthognathic surgery on osteoprotegerin as immunological caliper of bone healing. Open Access Maced J Med Sci 4: 705-708, 2016.
43. Reid PE, Brown NJ and Holen I: Breast cancer cells stimulate osteoprotegerin (OPG) production by endothelial cells through direct cell contact. Mol Cancer 8: 49, 2009.
44. Baud'huin M, Duplomb L, Teletchea S, Lamoureux F, Ruiz-Velasco C, Maillasson M, Redini F, Heymann MF and Heymann D: Osteoprotegerin: Multiple partners for multiple functions. Cytokine Growth Factor Rev 24: 401-409, 2013.
45. Bayer CM, Beckmann MW and Fasching PA: Updates on the role of receptor activator of nuclear factor κB/receptor activator of nuclear factor kappaB ligand/osteoprotegerin pathway in breast cancer risk and treatment. Curr Opin Obstet Gynecol 29: 4-11, 2017.
46. Zhang L, Liu M, Zhou X, Liu Y, Jing B, Wang X, Zhang Q and Sun Y: Role of osteoprotegerin (OPG) in bone marrow adipogenesis. Cell Physiol Biochem 40: 681-692, 2016.
47. Liu W, Xu C, Zhao H, Xia P, Song R, Gu J, Liu X, Bian J, Yuan Y and Liu Z: Osteoprotegerin induces apoptosis of osteoclasts and osteoclast precursor cells via the Fas/Fas ligand pathway. PLoS One 10: e0142519, 2015.
48. Kim CS, Bae EH, Ma SK, Han SH, Choi KH, Lee J, Chae DW, Oh KH, Ahn C and Kim SW; Representatives of the KNOW-CKD Investigator Group: Association of serum osteoprotegerin levels with bone loss in chronic kidney disease: Insights from the KNOW-CKD study. PLoS One 11: e0166792, 2016.
49. Van Poznak C, Cross SS, Saggese M, Hudis C, Panageas KS, Norton L, Coleman RE and Holen I: Expression of osteoprotegerin (OPG), TNF related apoptosis inducing ligand (TRAIL), and receptor activator of nuclear factor kappaB ligand (RANKL) in human breast tumours. J Clin Pathol 59: 56-63, 2006.
50. Ren H, Ren H, Li X, Yu D, Mu S, Chen Z and Fu Q: Effects of intermedin on proliferation, apoptosis and the expression of OPG/RANKL/M-CSF in the MC3T3-E1 osteoblast cell line. Mol Med Rep 12: 6711-6717, 2015.
51. Cheng Z, Landish B, Chi Z, Nannan C, Jingyu D, Sen L and Xiangjin L: 3D printing hydrogel with graphene oxide is functional in cartilage protection by influencing the signal pathway of Rank/Rankl/OPG. Mater Sci Eng C Mater Biol Appl 82: 244-252, 2018.